Supporting Information

Title: **The basolateral amygdala decodes visceral pain and itch via distinct circuits and molecules**

Qiuying Zhao[1, 2, #], Yong-Chang Li[2, #], Jia-He Yao[2, #], Rui-Xia Weng[1], Qianqian Chen[2], Xue Xu[3], Shufen Hu[2], Hong-Hong Zhang[4], Ying Zhang[3], Rui Li[1]*, Guang-Yin Xu[1, 2]**

	Ensembl ID	Gene name	Symbol (Description)	log_2FC	*p* value
	ENSMUSG00000040726	Hesx1	homeobox gene expressed in ES cells	7.159	0.000
	ENSMUSG00000087374	Gm15457	predicted gene 15457	5.817	0.003
	ENSMUSG00000102448	Gm37101	predicted gene, 37101	5.594	0.006
	ENSMUSG00000089628	Gm9727	predicted gene 9727	5.492	0.023
	ENSMUSG00000065760	Gm23848	predicted gene, 23848	5.358	0.027
	ENSMUSG00000037225	Fgf2	fibroblast growth factor 2	5.289	0.015
	ENSMUSG00000045275	Lca5l	Leber congenital amaurosis 5-like	5.212	0.033
	ENSMUSG00000072778	Vmn2r27	vomeronasal 2, receptor27	5.183	0.018
	ENSMUSG00000082580	Gm13182	predicted gene 13182	5.126	0.022
	ENSMUSG00000105322	Gm43751	predicted gene 43751	5.115	0.044
	ENSMUSG00000097832	Gm26912	predicted gene, 26912	5.049	0.049
	ENSMUSG00000116998	AC109266.1	genomic survey sequence of RP11-264P17 clone	5.042	0.026
	ENSMUSG00000004791	Pgf	placental growth factor	5.028	0.029
	ENSMUSG00000111922	Gm47760	predicted gene, 47760	5.016	0.028
	ENSMUSG00000104083	Gm29739	predicted gene, 29739	5.005	0.033
	ENSMUSG00000108478	Gm19514	predicted gene, 19514	4.931	0.038
CRD	ENSMUSG00000108251	Gm44112	predicted gene, 44112	4.913	0.039
	ENSMUSG00000035941	Ibtk	inhibitor of Bruton agammaglobulinemia tyrosine kinase	4.896	0.039
	ENSMUSG00000075570	Krt26	keratin 26	4.868	0.039
	ENSMUSG00000033323	Ctdp1	CTD (carboxy-terminal domain, RNA polymerase II, polypeptide A) phosphatase, subunit 1	4.855	0.042
	ENSMUSG00000009588	St6galnac1	ST6 (alpha-N-acetyl-neuraminyl-2,3-beta-galactosyl-1,3)-N-acetylgalactosaminide alpha-2,6-sialyltransferase	4.849	0.042
	ENSMUSG00000090326	Dthd1	death domain containing 1	4.815	0.044
	ENSMUSG00000031751	Amfr	autocrine motility factor receptor	4.527	0.026
	ENSMUSG00000068394	Cep152	centrosomal protein 152	4.450	0.025
	ENSMUSG00000032478	Nme6	NME/NM23 nucleoside diphosphate kinase 6	4.305	0.034
	ENSMUSG00000094958	3110021N24Rik	RIKEN cDNA clone-associated gene on mouse chromosome 11	4.284	0.039
	ENSMUSG00000074578	Zfas1	zinc finger, NFX1-type containing 1, antisense RNA 1	4.273	0.049
	ENSMUSG00000038015	Prm2	Cancer/testis antigen family 94, member 2	4.270	0.037
	ENSMUSG00000027935	Rab13	RAB13, member RAS oncogene family	4.190	0.046
	ENSMUSG00000032727	Mier3	MIER family member 3	4.105	0.030
	ENSMUSG00000050304	Slc25a2	solute carrier family 25 (mitochondrial carrier, ornithine transporter) member 2	21.816	0.000
	ENSMUSG00000040918	Slc19a2	solute carrier family 19 (thiamine transporter), member	21.392	0.000
	ENSMUSG00000010538	Tsacc	TSSK6 activating co-chaperone	21.070	0.000
	ENSMUSG00000117194	AC126254.2	genomic DNA sequence of RP23-398N16 clone on mouse chromosome 1	20.989	0.000
	ENSMUSG00000008822	Acyp1	acylphosphatase 1, erythrocyte (common) type	20.986	0.000
	ENSMUSG00000071178	Serpina1b	serine (or cysteine) preptidase inhibitor, clade A, member 1B	8.164	0.037
	ENSMUSG00000014543	Klra17	killer cell lectin-like receptor, subfamily A, member 17	8.161	0.037
	ENSMUSG00000037773	Pced1a	PC-esterase domain containing 1A	7.957	0.000
	ENSMUSG00000082109	Rpl19-ps12	ribosomal protein L19, pseudogene 12	7.677	0.050
	ENSMUSG00000021044	Adck1	aarF domain containing kinase 1	7.601	0.000
	ENSMUSG00000019850	Tnfaip3	tumor necrosis factor, alpha-induced protein 3	7.133	0.000
	ENSMUSG00000038917	3930402G23Rik	RIKEN cDNA 3930402G23 gene	6.915	0.000
	ENSMUSG00000094320	Chchd2-ps	coiled-coil-helix-coiled-coil-helix domain containing 2, pseudogene	6.818	0.000
	ENSMUSG00000020652	Cenpo	centromere protein O	6.760	0.001
His	ENSMUSG00000078773	Rad54b	RAD54 homolog B (S. cerevisiae)	6.664	0.002
	ENSMUSG00000094764	Olfr346	Olfactory receptor 1J5	6.498	0.013
	ENSMUSG00000044641	Pard6b	par-6 family cell polarity regulator beta	6.419	0.001
	ENSMUSG00000030188	Magohb	mago homolog B, exon junction complex core component	6.395	0.004
	ENSMUSG00000027878	Notch2	notch 2	6.375	0.002
	ENSMUSG00000030230	Plcz1	phospholipase C, zeta 1	6.112	0.002
	ENSMUSG00000062312	Erbb2	erb-b2 receptor tyrosine kinase 2	6.112	0.002
	ENSMUSG00000086537	Nespas	GNAS antisense RNA (Non-protein coding)	6.105	0.013
	ENSMUSG00000035275	Raver2	ribonucleoprotein, PTB-binding 2	6.026	0.013
	ENSMUSG00000018470	Kcnab3	potassium voltage-gated channel, shaker-related subfamily, beta member 3	5.959	0.010
	ENSMUSG00000028784	Spocd1	SPOC domain containing 1	5.912	0.012
	ENSMUSG00000050761	Gp1bb	glycoprotein Ib, beta polypeptide	5.859	0.013
	ENSMUSG00000098206	A430106G13Rik	RIKEN cDNA clone-associated gene on mouse chromosome 17	5.799	0.003
	ENSMUSG00000020412	Ascc2	activating signal cointegrator 1 complex subunit 2	5.722	0.003
	ENSMUSG00000022760	Thap7	THAP domain containing 7	5.618	0.008
	ENSMUSG00000037348	Paqr7	progestin and adipoQ receptor family member VII	5.582	0.007

Supplementary Table 1. The top DEGs of CRD-labeled group and His-labeled group. The table is divided into two parts: the upper part (green) lists

the 30 most significantly up-regulated genes in the CRD-labeled group，and the lower part (red) lists the 30 most significantly up-regulated genes in the His-labeled group. The key markers (circled in red in the table) include *Fgf2* and *Notch2*, which were validated as molecular identifiers of two functionally distinct BLA neurons selectively mediating visceral pain (CRD) and itch (His), respectively. Differential expression was analyzed using DESeq2 based on a negative binomial distribution and a two-tailed Wald test, $\log_2$ fold change > 4, *p* value < 0.05.

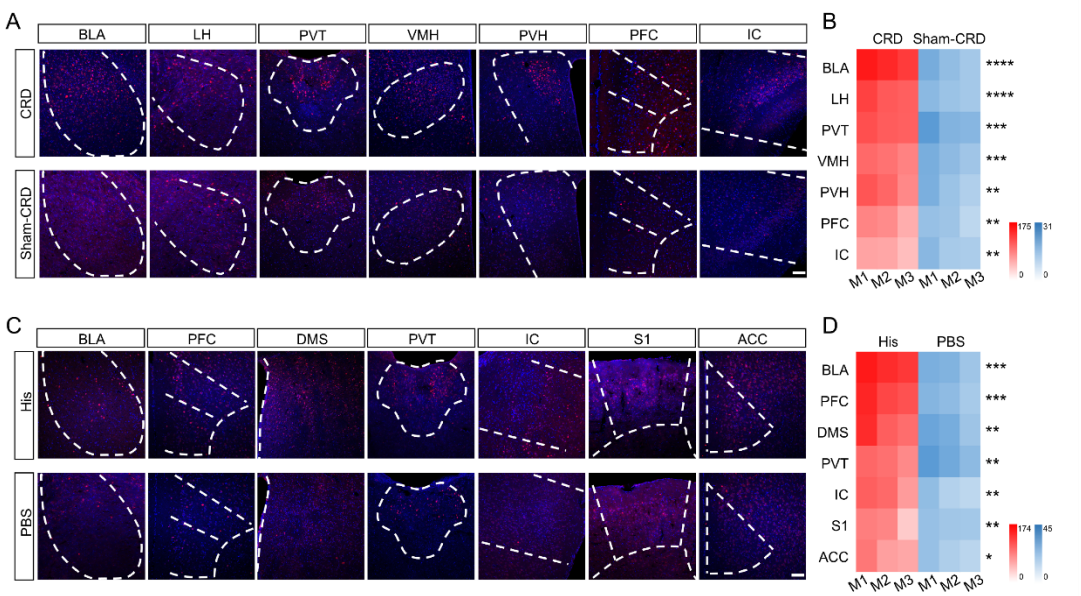

Fig. S1 Expression of CRD- and His-induced c-Fos in the BLA in female mice. (A) Representative immunofluorescence staining images showing c-Fos expression in the BLA, LH, PVT, VMH, PVH, PFC, IC of Sham-CRD and CRD mice. n = 3 mice, with two slices from each mouse. **(B)** Heatmap depicting of c-Fos expression in the BLA, LH, PVT, VMH, PVH, PFC, IC of Sham-CRD and CRD mice. n = 3 mice, with two slices from each mouse. ****P < 0.0001, ***P < 0.001, **P < 0.01, two-way ANOVA with Bonferroni test. n = 3 mice, two slices

from each mouse. **(C)** Representative immunofluorescence staining images showing c-Fos expression in the BLA, PFC, DMS, PVT, IC, S1, ACC of PBS and His mice. **(D)** Heatmap depicting of c-Fos expression in the BLA, PFC, DMS, PVT, IC, S1, ACC of PBS and His mice. n = 3 mice, with two slices from each mouse. ***P < 0.001, **P < 0.01, *P < 0.05, two-way ANOVA with Bonferroni test. n = 3 mice, two slices from each mouse. Scale bar = 100 μm in all panels.

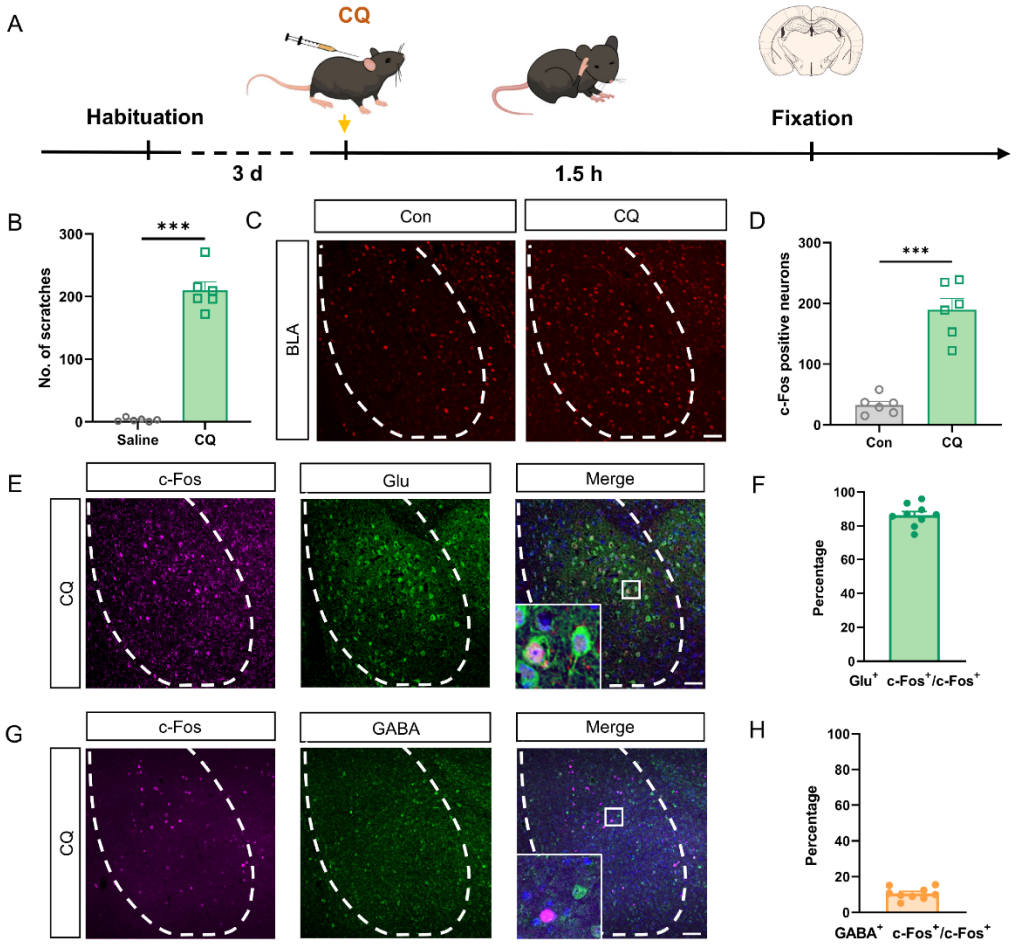

Fig. S2 Glutamatergic neurons in basolateral amygdala were activated in itch evoked by chloroquine. (A) Schematic timeline of the behavioral

experiment in itch evoked by chloroquine (CQ). **(B)** The number of scratching induced by CQ. ***P < 0.001, unpaired Student's t test, n = 6 mice. **(C)** Representative immunofluorescence images of c-Fos staining in BLA after the injection of saline or CQ into the nape. **(D)** Quantification of c-Fos-expressing neurons in response to CQ. ***P < 0.001, unpaired Student's t test, n = 6 brain sections from 3 mice per group. **(E-F)** Representative immunofluorescence images of BLA showing co-localization of glutamate and c-Fos (left) and the percentage of co-localization in the BLA (right), n = 9 brain sections from 3 mice per group. **(G-H)** Representative immunofluorescence images of BLA showing co-localization of GABA and c-Fos (left) and the percentage of co-localization in the BLA (right), n = 9 tissue sections from 3 mice per group. All data are presented as means ± SEM. Scale bar = 100 μm in all panels.

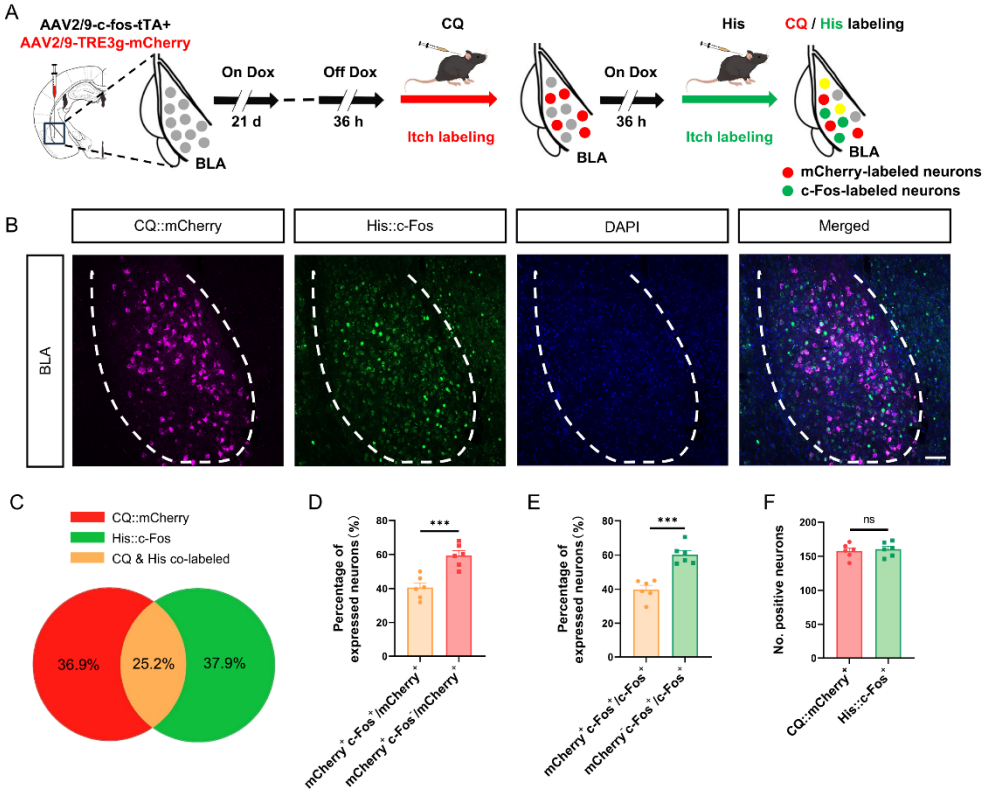

Fig. S3 Representation of CQ and His activated neural ensembles in the BLA. (A) Schematic illustration of the Tet-off viral system combined with c-Fos staining for labeling BLA neurons activated by CQ and His stimulation. **(B)** Representative images of BLA neurons activated by CQ and His, labeled with mCherry (red) and c-Fos (green), respectively. **(C)** Percentage of CQ-labeled neurons, His-labeled neurons, and CQ & His co-labeled neurons. **(D)** The proportion of mCherry^{+}c-Fos^{+} double-positive neurons relative to mCherry^{+} neurons was significantly lower than single-positive neurons. ***P < 0.001, paired Student's t test, n = 6 brain sections from 3 mice per group. **(E)** The proportion of mCherry^{+}c-Fos^{+} double-positive neurons relative to c-Fos^{+} neurons was significantly lower than single-positive neurons. ***P < 0.001, paired Student's t test, n = 6 brain sections from 3 mice per group. **(F)** Quantification of BLA neurons activated by CQ and His stimulation, n = 6 brain sections from 3 mice per group. All data are presented as means ± SEM. Scale bar = 100 μm in all panels, ns: no significance.

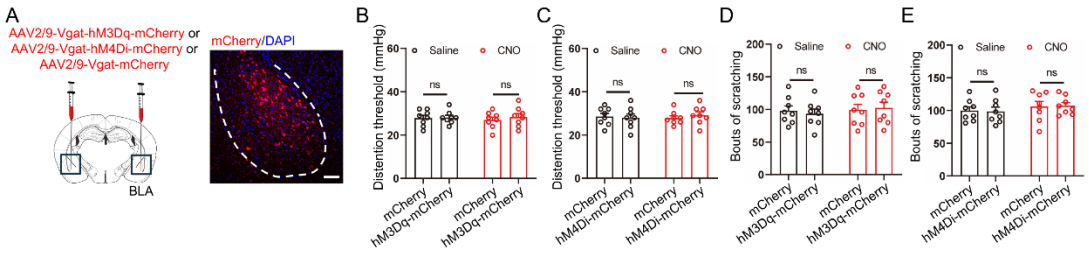

Fig. S4 Manipulation of BLA GABAergic neurons does not affect visceral pain or itch. (A) Schematic of the viral strategy and representative image showing the viral injection site in the BLA. **(B)** Chemogenetic activation of BLA GABAergic neurons does not affect visceral pain. **(C)** Chemogenetic inhibition

of BLA GABAergic neurons does not affect visceral pain. **(D)** Chemogenetic activation of BLA GABAergic neurons does not affect itch. **(E)** Chemogenetic inhibition of BLA GABAergic neurons does not affect itch. Two-way ANOVA followed by Bonferroni's post hoc test, n = 8 mice per group. Scale bar = 100 μm in all panels, ns: no significance.

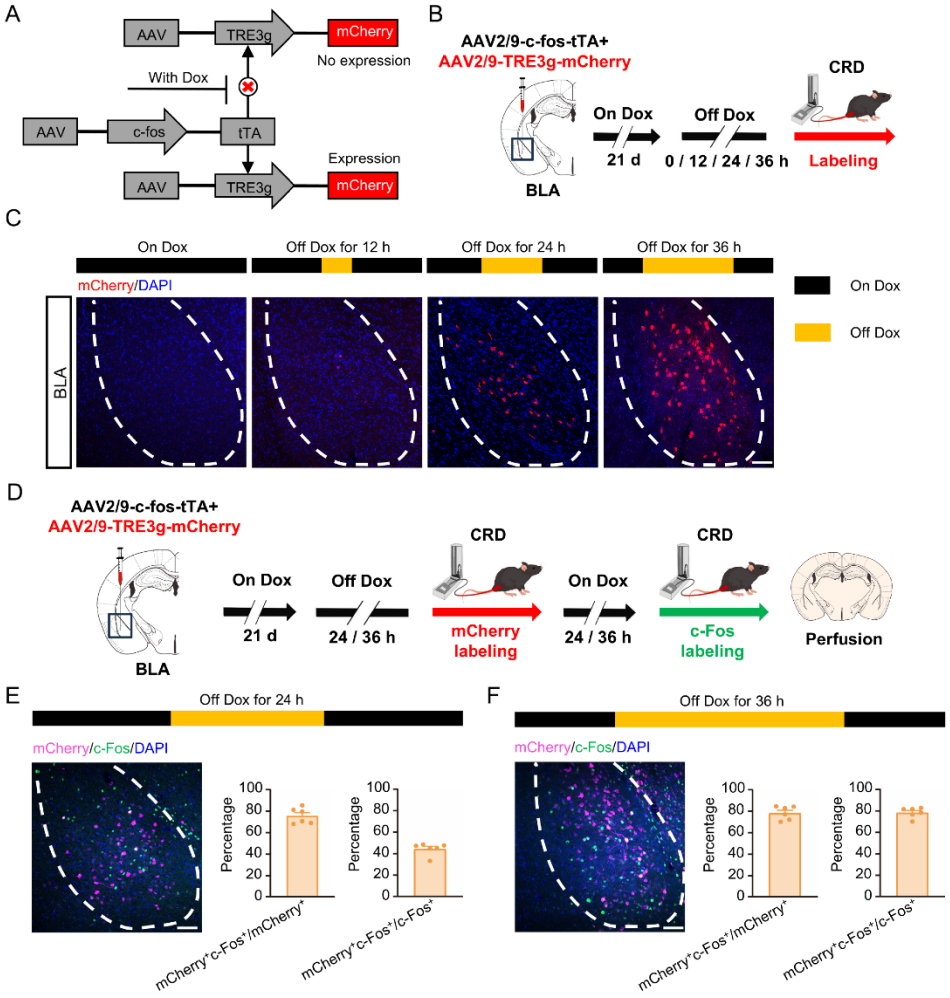

Fig. S5 Optimization of the time window for signal detection using the Tet-off system. (A) Schematic diagram illustrating the mechanism of the Tet-off viral system, wherein Dox-containing drinking water blocks the TRE3g promoter from functioning. **(B)** Schedule of evaluative experiments employing the Tet-off

system. **(C)** Representative images of mCherry expression during four different conditions. **(D)** Schematic for assessing the labeling efficiency and specificity of Tet-off system. **(E)** Representative images of BLA neurons activated by CRD labeled with mCherry (red) and c-Fos (green) for 24 h off dox (left), labelling efficiency and specificity of Tet-off system for 24 h off dox (right), n = 6 brain sections from 3 mice per group. **(F)** Representative images of BLA neurons activated by CRD labeled with mCherry (red) and c-Fos (green) for 36 h off dox (left), labelling efficiency and specificity of Tet-off system for 36 h off dox (right), n = 6 brain sections from 3 mice per group. All data are presented as means ± SEM. Scale bar = 100 μm in all panels.

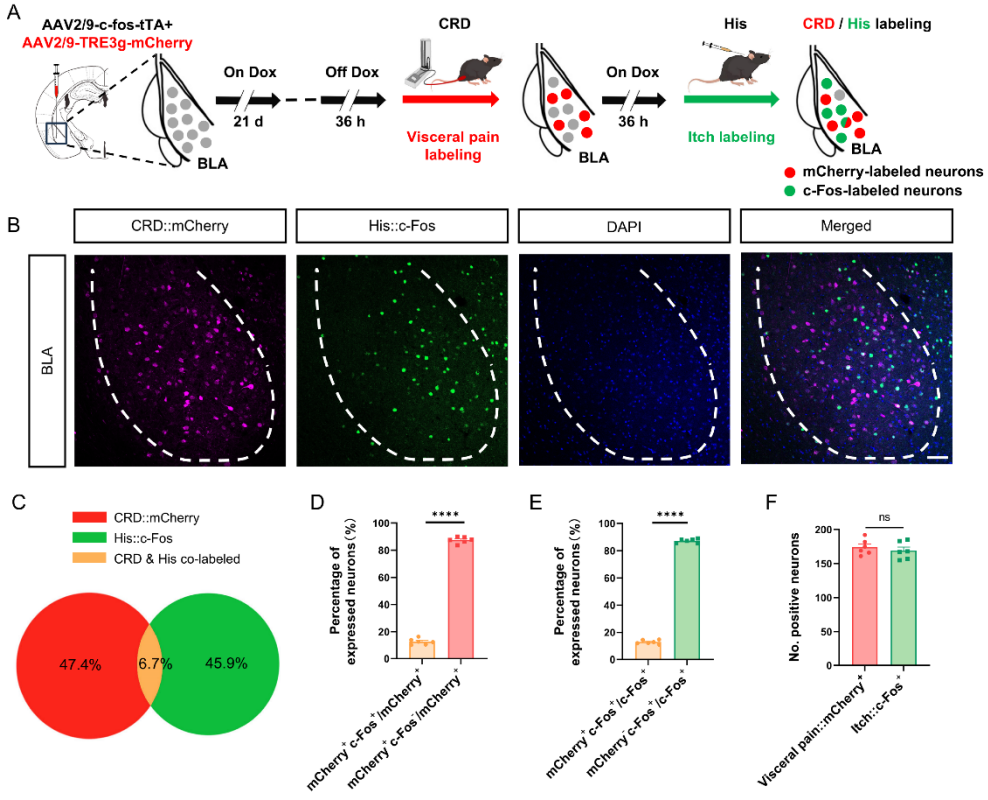

Fig. S6 CRD and His activated neurons are two distinct ensembles in BLA.

(A) Schematic illustration of the Tet-off viral system combined with c-Fos

staining for labeling BLA neurons activated by CRD and His stimulation. **(B)** Representative images of BLA neurons activated by CRD and His, labeled with mCherry (red) and c-Fos (green), respectively. **(C)** Percentage of CRD-labeled neurons, His-labeled neurons, and CRD & His co-labeled neurons. **(D)** The proportion of mCherry^{+}c-Fos^{+} double-positive neurons relative to mCherry^{+} neurons was significantly lower than single-positive neurons. ****P < 0.0001, paired Student's t test, n = 6 brain sections from 3 mice per group. **(E)** The proportion of mCherry^{+}c-Fos^{+} double-positive neurons relative to c-Fos^{+} neurons was significantly lower than single-positive neurons. ****P < 0.0001, paired Student's t test, n = 6 brain sections from 3 mice per group. **(F)** Quantification of BLA neurons activated by CRD and His stimulation, paired Student's t test, n = 6 brain sections from 3 mice per group. All data are presented as means ± SEM. Scale bar = 100 μm in all panels, ns: no significance.

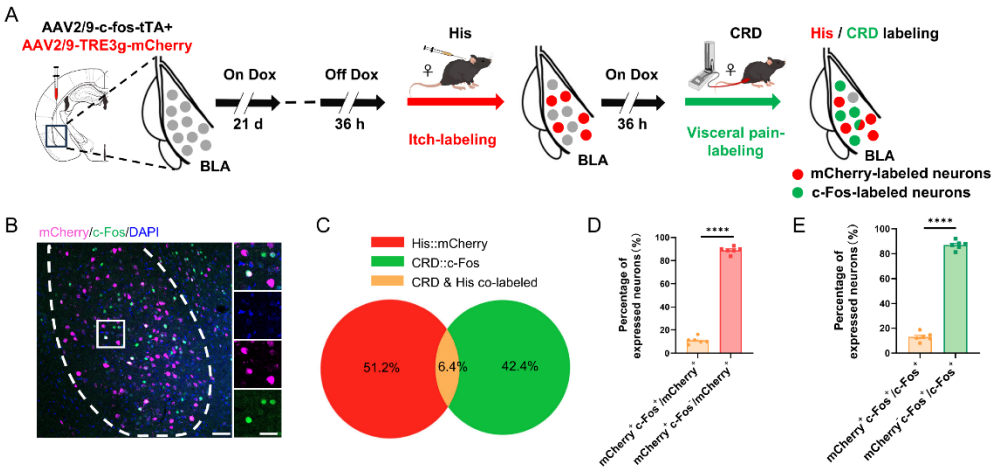

Fig. S7 His and CRD activated neurons are two distinct ensembles in BLA in female mice. (A) Schematic illustration of the Tet-off viral system combined with c-Fos staining for labeling BLA neurons activated by His and CRD

stimulation. **(B)** Representative images of BLA neurons activated by His and CRD, labeled with mCherry (red) and c-Fos (green), respectively. Scale bar = 100 μm, scale bar = 50 μm in zoomed image. **(C)** Percentage of His-labeled neurons, CRD-labeled neurons, and CRD & His co-labeled. **(D)** The proportion of mCherry$^+$c-Fos$^+$ double-positive neurons relative to mCherry$^+$ neurons was significantly lower than single-positive neurons. ****P < 0.0001, paired Student's t test, n = 6 brain sections from 3 mice per group. **(E)** The proportion of mCherry$^+$c-Fos$^+$ double-positive neurons relative to c-Fos$^+$ neurons was significantly lower than single-positive neurons. ****P < 0.0001, paired Student's t test, n = 6 brain sections from 3 mice per group. All data are presented as means ± SEM.

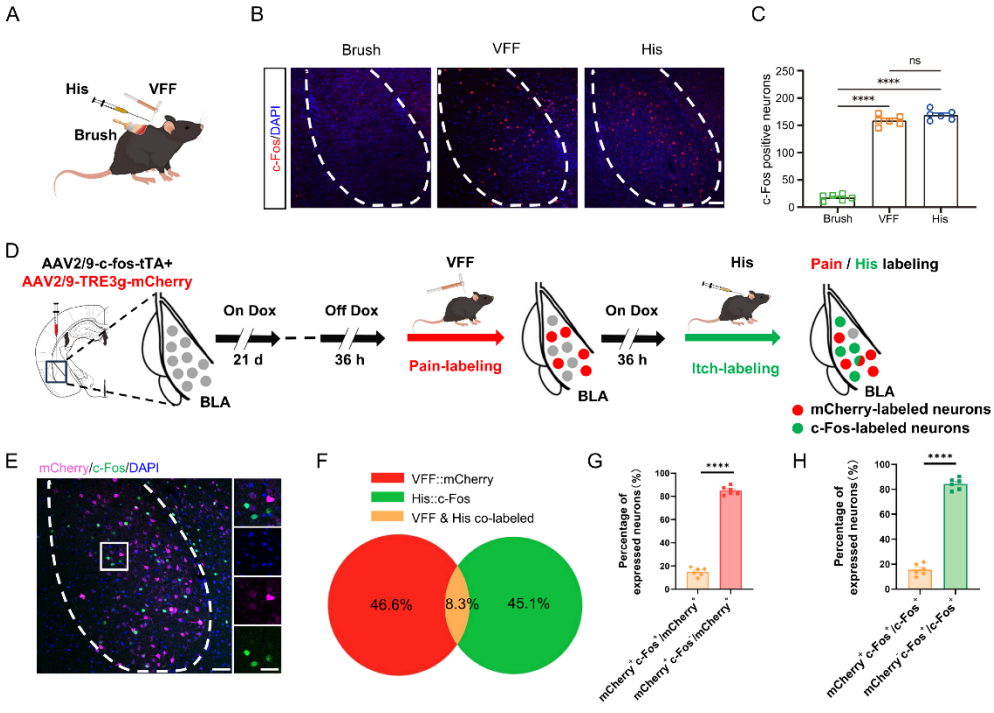

Fig. S8 The distinction between somatic pain and itch in the BLA is independent of topographical location. (A) Schematic of the experimental

paradigm for c-Fos expression following VFF, His, and non-nociceptive brush stimulation applied to the back. **(B)** Representative immunofluorescence staining images showing c-Fos expression of non-nociceptive brush, VFF, and His stimulation. Scale bar =100 μm. **(C)** Quantification of c-Fos-expressing neurons in response to non-nociceptive brush, VFF, and His stimulation. ****$P < 0.0001$, one-way ANOVA followed by Turkey's post hoc test, n = 6 brain sections from 3 mice per group, ns: no significance. **(D)** Schematic illustration of the Tet-off viral system combined with c-Fos staining for labeling BLA neurons activated by VFF (pain) and His (itch) stimulation applied to the back. **(E)** Representative images of BLA neurons activated by VFF and His, labeled with mCherry (red) and c-Fos (green), respectively. Scale bar = 100 μm, scale bar = 50 μm in zoomed image. **(F)** Percentage of VFF-labeled neurons, His-labeled neurons, and VFF & His co-labeled neurons. **(G)** The proportion of $mCherry^+c\text{-}Fos^+$ double-positive neurons relative to $mCherry^+$ neurons was significantly lower than single-positive neurons. ****$P < 0.0001$, paired Student's t test, n = 6 brain sections from 3 mice per group. **(H)** The proportion of $mCherry^+c\text{-}Fos^+$ double-positive neurons relative to $c\text{-}Fos^+$ neurons was significantly lower than single-positive neurons. ****$P < 0.0001$, paired Student's t test, n = 6 brain sections from 3 mice per group. All data are presented as means ± SEM.

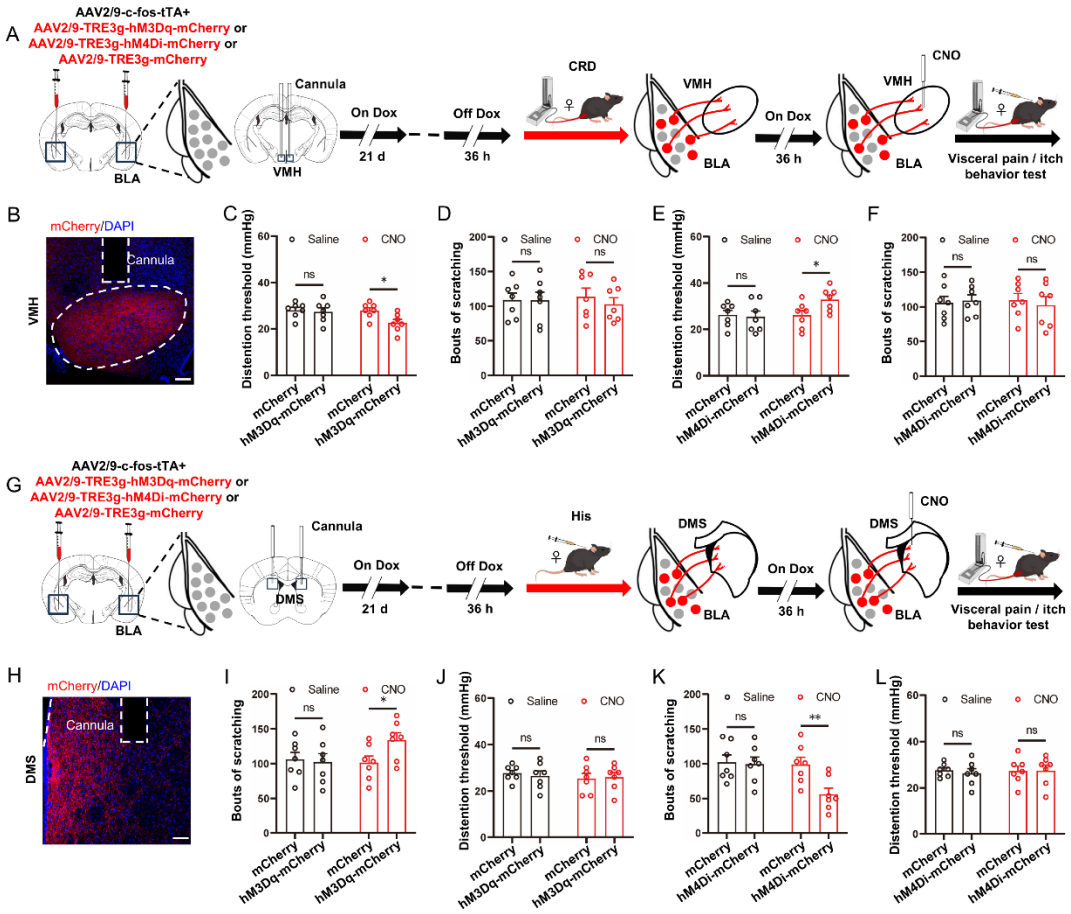

Fig. S9 Manipulation of the projections from CRD-labeled BLA neurons to VMH or His-labeled BLA neurons to DMS specifically modulates visceral pain or itch behaviors in female mice. (A) Schematic of the viral strategy and experimental timeline for manipulating the projections of CRD-labeled BLA neural ensembles to the VMH. **(B)** Representative immunofluorescence images of axonal terminals in the VMH. **(C-D)** Chemogenetic activation of the projections of CRD-labeled BLA neural ensembles to the VMH significantly reduces the visceral pain threshold (C) without affecting itch (D). **P* < 0.05, two-way ANOVA followed by Bonferroni's post hoc test, n = 7 mice per group. **(E-F)** Chemogenetic inhibition of the projections of CRD-labeled BLA neural ensembles to the VMH significantly increases visceral pain threshold (E) without affecting itch (F). **P* < 0.05, two-way ANOVA followed by Bonferroni's

post hoc test, n = 7 mice per group. **(G)** Schematic of the viral strategy and experimental timeline for manipulating the projections of His-labeled BLA neural ensembles to the DMS. **(H)** Representative immunofluorescence images of axonal terminals in the DMS. **(I-J)** Chemogenetic activation of the projections of His-labeled BLA neural ensembles to the DMS significantly increases the bouts of scratching (I) without affecting visceral pain (J). $^{**}P < 0.01$, two-way ANOVA followed by Bonferroni's post hoc test, n = 7 mice per group. **(K-L)** Chemogenetic inhibition of the projections of His-labeled BLA neural ensembles to the DMS significantly reduces the bouts of scratching (K) but had no effect on visceral pain (L). $^{*}P < 0.05$, two-way ANOVA followed by Bonferroni's post hoc test, n = 7 mice per group. Scale bar = 100 μm in all panels, ns: no significance.

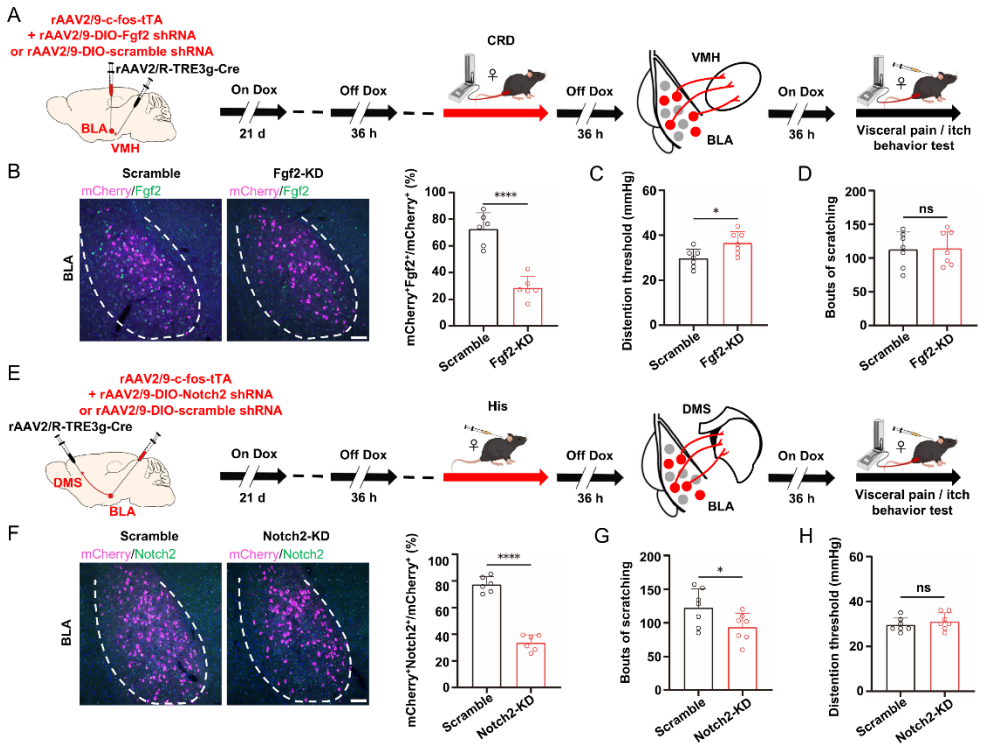

Fig. S10 Knockdown of Fgf2 in CRD-labeled BLA neurons projecting to

VMH attenuates visceral pain whereas knockdown of Notch2 in His-labeled BLA neurons projecting to DMS inhibits itch in female mice. (A) Schematic of the viral strategy and experimental timeline for specifically knocking down *Fgf2* in CRD-labeled BLA neurons projecting to the VMH. **(B)** Representative images showing knockdown of Fgf2 and the corresponding statistical graphs. ****$P < 0.0001$, unpaired Student's t test, n = 6 brain sections from 3 mice per group. **(C-D)** Knockdown of *Fgf2* specifically increases visceral pain threshold (C) without affecting itch (D). *$P < 0.05$, unpaired Student's t test, n = 8 mice per group. **(E)** Schematic of the viral strategy and experimental timeline for specifically knocking down *Notch2* in His-labeled BLA neurons projecting to the DMS. **(F)** Representative images showing knockdown of Notch2 and the corresponding statistical graphs. ****$P < 0.0001$, unpaired Student's t test, n = 6 brain sections from 3 mice per group. **(G-H)** Knockdown of *Notch2* specifically decreases the bouts of scratching (G) without affecting visceral pain (H). *$P < 0.05$, unpaired Student's t test, n = 8 mice per group. Scale bar =100 μm in all panels, ns: no significance. All data are presented as means ± SEM.